J. Math. Computer Sci., 31 (2023), 461–476

Online: ISSN 2008-949X

Journal of Mathematics and Computer Science

Journal Homepage: www.isr-publications.com/jmcs

Dynamics of a mathematical model of oncolytic virotherapy with tumor-Virus interaction

Abdullah Abu-Rqayiq[a,*], Haneen Alayed[b]

[a]Concord University, Athens, WV, 24712, USA.

[b]New Mexico State University, Las Cruces, NM, 88001, USA.

Abstract

Virotherapy is a cancer treatment that uses a virus that can target cancer cells to infect, replicate, and destroy them leaving the healthy cells unharmed. Recently, considerable efforts have been made to understand the mechanisms and dynamics of oncolytic virotherapy. In this paper, we study the dynamics of a basic model of oncolytic tumor virotherapy. This model emphasizes the interaction between cancer-infected cells and cancer uninfected cells. To understand some of the consequences of this contact from a mathematical point of view, we study the dynamics behavior of the model and present a qualitative analysis of the equilibria. To illustrate which parameters in the model affect the outcome of virotherapy the most, we determine bifurcation parameters and conduct a sensitivity analysis of the model's parameters. Numerical simulations are conducted to show the validity of our analysis.

Keywords: Cancer, oncolytic virotherapy, stability, Lyapunov, basic reproductive number.

2020 MSC: 92C50, 93A30, 37N35, 34K28.

1. Introduction

Since the late 1880s, viruses have attracted considerable interest as possible agents of tumor destruction. The history of oncolytic viruses tells us that doctors have observed that some cancer patients do go into remission after viral infection [15]. Since then, the approach of using viruses in tumor therapy has gained considerable interest and still occupies a noticeable interest of researchers for cancer therapy. The main question that most of the researchers tried to address for a long time was how to eliminate the pathogenicity of those viruses so that they become suitable as drugs. It was found that under the right circumstances, viruses are capable of destroying tumor tissue in human cancer patients. In the meantime, it was found that the damage inflicted on tumor tissues is far more significant than the damage inflicted on normal host tissues. Due to their pathogenicity, most of these viruses were not considered safe for cancer therapy. However, thanks to adaptation and genetic engineering techniques, the pathogenicity can be eliminated in most of the viruses without destroying their oncolytic potency [15]. This therapy using selected viruses that can specifically target cancer cells is known as oncolytic virotherapy.

*Corresponding author

Email address: aaburqayiq@concord.edu (Abdullah Abu-Rqayiq)

doi: 10.22436/jmcs.031.04.08

Received: 2023-03-15 *Revised:* 2023-03-31 *Accepted:* 2023-05-10

Oncolytic virotherapy is a form of immunotherapy that uses certain viruses to attack, infect, replicate, and destroy tumor cells. The idea is that when free viruses infect tumor cells they replicate themselves in those cells; upon breaking down infected tumor cells, new virion particles burst out and proceed to infect additional tumor cells. In this treatment, viruses can selectively replicate only in cancer cells but leave healthy normal cells largely intact. The new viruses released from the lysed cells can subsequently infect adjacent or distant tumor cells and trigger multiple cycles of infection. Recently, great efforts have been made for understanding the dynamics and molecular mechanics of viral cytotoxicity of oncolytic viruses. Those efforts provided an interesting possible alternative therapeutic approach to help cure cancer patients. However, the outcomes of virotherapy depend in a complex way on the virus-cancer interaction as well as the immune response. ([5, 7, 8, 20, 23])

Most of the clinically used cancer therapies have been developed empirically [11]. However, many mathematical models have been recently developed to describe the outcome of such interaction ([3–12, 28, 33]). More models and different approaches are also developed to study the dynamics of virotherapy ([1, 2, 13, 20, 22, 23, 27–30]). Several mathematical models of virotherapy have been formulated using some classical mathematical models such Lotka-Volterra models, and reaction-diffusion models. These models usually assume that populations are well-mixed. However, this may not be the case as it is evident, see for example [9], that the spacial component and local interactions are very important to population growth.

Many current modeling approaches have generally lacked any experimental data to validate them. To address this problem, [4, 5] have developed an in silico computational model that can describe the dynamics between the tumor and virus populations in a spatially explicit manner. They used in vitro 2D and 3D data to inform the model parameters and then use the computational model to explore various critical properties of oncolytic viruses. They showed that the introduction of a third dimension alters the dynamics significantly and that this has important implications for the outcome of therapy. However, their study lacked the investigation of the mathematical qualitative properties of the model.

In this paper, we study the qualitative properties of the model from [4, 5] and we investigate the stability of equilibrium points and describe the behavior of the solution. The model has significant aspects that make it interesting, both mathematically and clinically. For instance, the model has an abundance of equilibria. Specifically, it has five equilibrium points which make dynamic behavior more complicated from one side, and rich and interesting from the other side. Clinically, the model allows for a more realistic study of the dynamics of oncolytic viruses, as it can depict the case in which populations of cancer and virus cannot move freely throughout the environment.

In addition to investigating the stability of the equilibrium points, we conduct a sensitivity analysis of the model to show the effect and weight of each parameter in determining the dynamics. We also carry out numerical simulations to prove our theoretical results. The obtained results were compared to the results in the literature and provide a comprehensive mathematical analysis of the cancer-virus interaction.

The paper is organized as follows. In Section 2, the mathematical model is introduced and parameters are described. In Section 3 mathematical proofs of the important qualitative properties of the model are presented. In Section 4, numerical simulations and sensitivity analysis of the model are conducted. Finally, in Section 5 conclusions and discussions are provided.

2. Mathematical model

The model under consideration is a classical 3-species Lotka-Volterra system, those systems have played a significant role in modeling the competition between species, which has a great impact on studying different competition models in biology, ecology, and medicine. See, for instance, [13, 14, 24]. In our model, three types of cells are involved: normal cells denoted as x, cancer cells y, and infected cancer cells v. This model is a mean-field model based on predator-prey interactions, and it describes the interaction between tumor growth and viral infection of tumor cells. Despite the fact that the significant

Table 1: Pameters' description, ref. [4].

Parameter	Description	Value	Unit
r	Proliferation of normal cells	0.5	$1/h$ cell
a	Death rate of normal population	0.2	$1/h$ cell
s	Proliferation of the uninfected cells	1.0	$mm^3h/$ cell
b	Death rate of uninfected population	0.1	$1/h$ cell
c	Proliferation of the infected cells	1.2	$mm^3h/cell$
d	Death rate of the infected cells	0.1	$1/h$ cell

interaction is mainly between infected and uninfected cells, the normal cells can be spatially affected by this competition. Therefore, the three model compartments can capture the basic dynamics of such interaction.

The model is formulated using the following scenario: A network with nodes occupied with the three types of cells as well as empty ones can be used to model the virotherapy under consideration. When a normal cell or cancer cell proliferates, the newly generated cell has to occupy a nearby empty node while infected cells can only attack and occupy a node resided by a cancer cell as the virus is programmed to attack only cancer cells, and the virus spreads from cell to cell ([18, 21]). Arrival times of the viruses vary but follow the Poisson process with time to the next event being exponentially distributed. The model assumes that the growth and death rates of the three types of cells can be varied. Also, virus infection parameters can be specified ([4, 5]).

The model, described above, is governed by the following system of differential equations, where all of the parameters are nonnegative:

$$\frac{dx}{dt} = rx\,(1-x-y-v) - ax, \quad \frac{dy}{dt} = sy\,(1-x-y-v) - by - cyv, \quad \frac{dv}{dt} = cyv - dv. \tag{2.1}$$

The initial values assumed in the model (2.1) are

$$x(0) \geqslant 0, \quad y(0) \geqslant 0, \text{ and } \quad v(0) \geqslant 0,$$

where r represents the proliferation and a, b, and d represent the death rates of the respective populations. The model assumes mass action kinetics and was fitted to data from in vitro studies ([4, 5]).

3. Qualitative analysis

In this section, we investigate the basic qualitative properties of the model (2.1) at the biologically feasible equilibria. We prove the positivity and boundedness of solutions in a specific invariant domain. Then we obtain steady-state solutions of the model and study their stability.

3.1. Positivity and boundedness

Theorem 3.1. *All solutions of the system (2.1) are nonnegative and bounded in the invariance region with nonnegative initial conditions in the region*

$$\Omega = \{(x, y, v) \in \mathbb{R}^3_+ : x \leqslant 1, y + v \leqslant 1\}.$$

Proof. We show the nonnegativity of solutions first. Rewrite the first equation of model (2.1) as

$$\frac{dx}{x} = \phi_1(x, y, v)dt,$$

where $\phi_1(x, y, v) = r(1 - x - y - v) - a$. By integrating over $[0, t]$, we obtain

$$x(t) = x(0)\exp\Big[\int_0^t \phi_1(x, y, v)ds\Big].$$

Since $x(0) \geqslant 0$, we have $x(t) \geqslant 0$ for all $t \geqslant 0$. From the second equation of model (2.1) we can write

$$\frac{dy}{y} = \phi_2(x, y, v)dt,$$

where $\phi_2(x, y, v) = s(1 - x - y - v) - b - cv$. By integrating over $[0, t]$, we obtain

$$y(t) = y(0) \exp\left[\int_0^t \phi_2(x, y, v)ds\right].$$

Since $y(0) \geqslant 0$, we have $y(t) \geqslant 0$ for all $t \geqslant 0$. From the third equation of model (2.1) we can write

$$\frac{dv}{v} = \phi_3(x, y, v)dt,$$

where $\phi_3(x, y, v) = cy - d$. By integrating over $[0, t]$, we obtain

$$v(t) = v(0) \exp\left[\int_0^t \phi_3(x, y, v)ds\right].$$

Since $v(0) \geqslant 0$, we have $v(t) \geqslant 0$ for all $t \geqslant 0$. Hence, the solutions $x(t), y(t)$, and $v(t)$ are nonnegative for nonnegative initial data.

Now we prove that all solutions are bounded. Consider the initial value problem

$$\frac{dW}{dt} = rW(1 - W), \quad W(0) = W_0. \tag{3.1}$$

The solution to (3.1) is given by

$$W(t) = \frac{W_0}{W_0 + (1 - W_0)e^{-rt}}.$$

Note that $\limsup_{t \longrightarrow \infty} W(t) \leqslant 1$, and also $\frac{dx}{dt} \leqslant \frac{dW}{dt}$. Thus, $\limsup_{t \longrightarrow \infty} x(t) \leqslant \limsup_{t \longrightarrow \infty} W(t) = 1$. Therefore, $x(t)$ is bounded. Similarly, note that

$$\frac{dy}{dt} + \frac{dv}{dt} = sy(1 - x - y - v) - by - dv \leqslant s(1 - (y + v)).$$

Thus, $y(t) + v(t) \leqslant 1$. Hence, $\limsup_{t \longrightarrow \infty} y(t) + v(t) \leqslant 1$. Therefore, all the solutions to the model (2.1) are bounded in the invariant domain Ω. □

3.2. *Equilibria and basic reproduction number*

The equilibrium points of the system are the steady-state solutions. Model (2.1) has five equilibrium points as follows.

(i) The trivial equilibrium $E_0 = (0, 0, 0)$: represents a free equilibrium where all populations die out.
(ii) The cancer extinction equilibrium $E_1 = (1 - \mu_1, 0, 0)$: once cancer is extinct, the infected cells will follow if their death rate is positive.
(iii) The virus extinction equilibrium $E_2 = (0, 1 - \mu_2, 0)$: the virus population reaches zero which implies that normal cells are also extinct.
(iv) The cancer-virus equilibrium $E_3 = (0, \frac{d}{c}, \frac{sc - bc - ds}{s + c})$: normal cells die out leaving cancer cells and virus-infected cells with stable sizes.
(v) Three population equilibrium $E_4 = (\frac{c(r - a) - r(d + b) - as}{rc}, \frac{d}{c}, \frac{as}{rc} - \frac{b}{c})$: all three cell types are present and have stable population sizes.

Where for simplicity of calculations and emphasizing the important parameters through the study, we denote $\mu_1 = \frac{a}{r}$, and $\mu_2 = \frac{b}{s}$.

The basic reproduction number denoted by $\mathcal{R}_0$, can be considered as the number of secondary cases of infection generated from a single virus in a population where all tumor cells are susceptible to infection. Applying the Next Generation Method, let $\mathcal{P} = (x, y, v)$, then model (2.1) can be rewritten as $\mathcal{P}' = \tilde{F}(\mathcal{P}) - \tilde{V}(\mathcal{P})$, where the matrices $\tilde{F}$ and $\tilde{V}$ represent respective new infection and transition, and they are given by

$$\tilde{F}(\mathcal{P}) = \begin{pmatrix} 0 \\ 0 \\ cyv \end{pmatrix} \quad \text{and} \quad \tilde{V}(\mathcal{P}) = \begin{pmatrix} -rx(1-x-y-v)+ax \\ -sy(1-x-y-v)+by+cyv \\ dv \end{pmatrix}.$$

Now, evaluating the Jacobian matrices associated with the above two matrices at the virus extinction equilibrium E_2, where all tumor cells are uninfected, we obtain

$$J(\tilde{F}(E_2)) = \begin{pmatrix} 0 & 0 & 0 \\ 0 & 0 & 0 \\ 0 & 0 & c(1-\frac{b}{s}) \end{pmatrix} \quad \text{and} \quad J(\tilde{V}(E_2)) = \begin{pmatrix} a-\frac{rb}{s} & 0 & 0 \\ s-b & b-s & s-b+c-\frac{cb}{s} \\ 0 & 0 & d \end{pmatrix}.$$

We denote $F = J(\tilde{V}(E_2))$ and $V = J(\tilde{V}(E_2))$. Applying the next-generation matrix [28], we obtain

$$FV^{-1} = \begin{pmatrix} 0 & 0 & 0 \\ 0 & 0 & 0 \\ 0 & 0 & \frac{c(s-b)}{sd} \end{pmatrix}.$$

Then, we find that the basic reproduction number $\mathcal{R}_0$ is given by $\mathcal{R}_0 = \rho(FV^{-1}) = \frac{c(s-b)}{sd}$, where $\rho(FV^{-1})$ denotes the spectral radius of matrix FV^{-1}.

The importance of $\mathcal{R}_0$ in the control of disease dynamics is evident from the extensive efforts to estimate its value for various diseases and its role in the study of the dynamics of the disease [16].

3.3. Local stability analysis

In this section, we investigate the local stability of the equilibrium points of the model (2.1). We start our qualitative analysis by finding the Jacobian matrix of the model. This is given by

$$J = \begin{pmatrix} r(1-2x-y-v)-a & -rx & -rx \\ -sy & s(1-x-2y-v)-b-cv & -sy-cy \\ 0 & cv & cy-d \end{pmatrix}.$$

Our main local stability results are summarized in the following theorem.

Theorem 3.2. *For the system (2.1), the local behavior of the equilibria can be described as follows.*

(i) *The equilibrium point* E_0 *is locally asymptotically stable if* $\mu_1 > 1$ *and* $\mu_2 > 1$.
(ii) *The equilibrium point* E_1 *is locally asymptotically stable if* $\mu_1 < 1$ *and* $\mu_2 < 1$.
(iii) *The equilibrium point* E_2 *is locally asymptotically stable if* $\mu_2 < 1$, $\mu_2 < \mu_1$, *and* $\mathcal{R}_0 < 1$.
(iv) *The equilibrium point* E_3 *is locally asymptotically stable if* $\mu_1 > 1$ *and* $d > b$, *and* $AB - C > 0$, *where* A, B, *and* C *are the coefficient of the associated characteristic polynomial.*
(v) *The equilibrium point* E_4 *is locally asymptotically stable if* $\frac{s+2b}{s+4b} < \frac{\mu_1}{\mu_2} < \frac{d-b}{a-b}$ *and* $\frac{c(r-a)}{r(d-b)+s(a-d)} > 1$.

Proof.

(i) The Jacobian matrix evaluated at the disease-free equilibrium point is given by

$$J(E_0) = \begin{pmatrix} r-a & 0 & 0 \\ 0 & s-b & 0 \\ 0 & 0 & -d \end{pmatrix}.$$

Since the matrix is upper triangular, the eigenvalues are the entries of the main diagonal. Hence, the

eigenvalues are negative when $\mu_1 > 1$ and $\mu_2 > 1$.

(ii) The Jacobian matrix evaluated at E_1 is given by

$$J(E_1) = \begin{pmatrix} a-r & a-r & a-r \\ 0 & \frac{sa}{r} - b & 0 \\ 0 & 0 & -d \end{pmatrix}.$$

The eigenvalues of this upper triangular matrix are $a-r$, $\frac{sa}{r} - b$, and $-d$. They are negative if $\mu_1 < \mu_2$ and $\mu_1 < 1$.

(iii) The Jacobian matrix evaluated at E_2 is given by

$$J(E_2) = \begin{pmatrix} \frac{rb}{s} - a & 0 & 0 \\ b-s & b-s & b-s-c+\frac{bc}{s} \\ 0 & 0 & c-d-\frac{bc}{s} \end{pmatrix}.$$

The eigenvalues are $\lambda_1 = \frac{rb}{s} - a$, $\lambda_2 = b-s$, and $\lambda_3 = c-d-\frac{bc}{s}$. These eigenvalues are all negative if $a > \frac{rb}{s}$, $s > b$, and $c-d-\frac{bc}{s} < 0$. Hence, the stability conditions are $\mu_2 < \mu_1$, $\mu_2 < 1$, and $\mathcal{R}_0 < 1$.

(iv) The Jacobian matrix evaluated at E_3 is given by

$$J(E_3) = \begin{pmatrix} \frac{r(c-d+b)}{c+s} - a & 0 & 0 \\ -\frac{sd}{c} & -\frac{sd}{c} & -\frac{sd}{c} - d \\ 0 & \frac{sc-bc-ds}{c+s} & 0 \end{pmatrix}.$$

The characteristic polynomial is given by

$$\lambda^3 + A\lambda^2 + B\lambda + C = 0,$$

where

$$\begin{aligned}
A &= \frac{sd}{c} - \frac{rb-rd+rc}{c+s} + a, \\
B &= \frac{s^2dc - sbdc - s^2d^2 + sdc - bcd - d^2s - rsbd - rsd}{c+s} + \frac{asd}{c} + \frac{rd^2s}{c(c+s)}, \\
C &= \frac{rsbdc^2 - rs^2dc^2 + 2rs^2cd^2 - rsc^2d + rc^2bd + 2rscd^2 - rsbcd^2 - rs^2d^3 - rd^2bc - rsd^3}{(c+s)^2} \\
&\quad - \frac{rs^2bcd + rsb^2cd + rs^2bd^2 - rsbcd + rb^2cd + rsbd^2 + as^2dc^2 + as^3dc - asbc^2d - as^2bcd}{(c+s)^2} \\
&\quad - \frac{acs^2d^2 - as^3d^2 + asdc^2 + as^2cd - abc^2d - sabcd - acd^2s - s^2ad^2}{(c+s)^2}.
\end{aligned}$$

By the Routh-Hurwitz criterion, all roots of the characteristic equation have negative real parts if and only if $A > 0$ and $AB - C > 0$. The first condition is satisfied if $\mu_1 > 1$ and $d > b$. The two conditions imply the stability of the equilibrium point E_3.

(v) The Jacobian matrix evaluated at E_4 is given by

$$J(E_4) = \begin{pmatrix} \frac{c(a-r)+r(d-b)+as}{c} & \frac{c(a-r)+r(d-b)+as}{c} & \frac{c(a-r)+r(d-b)+as}{c} \\ -\frac{sd}{c} & -\frac{sd}{c} & -\frac{sd}{c} - d \\ 0 & \frac{sa}{r} - b & 0 \end{pmatrix}.$$

The characteristic equation is given by

$$\lambda^3 + A\lambda^2 + B\lambda + C = 0.$$

Where

$$A = r - a - \frac{rd}{c} + \frac{rb}{c} - \frac{as}{c} + \frac{sd}{c},$$
$$B = (\frac{bds}{c} + bd)(\frac{as}{br} - 1),$$
$$C = abd + sad - rbd - \frac{s^2a^2d}{cr} - \frac{sa^2d}{r} - \frac{sad^2}{c} + \frac{rbd^2}{c} - \frac{2sabd}{c} + \frac{rb^2d}{c}.$$

By the Rough-Hurwitz criterion, all roots of the equation have negative real parts if and only if $A > 0$ and $AB - C > 0$. The first condition, $A > 0$ holds if $\frac{c(r-a)}{r(d-b)+s(a-d)} > 1$. The condition $AB - C > 0$ holds if $\frac{b(s+2b)}{s(s+4b)} < \frac{a}{r} < \frac{b(d-b)}{s(a-b)}$. Hence, the conditions under which the equilibrium E_4 is locally asymptotically stable are

$$\frac{s+2b}{s+4b} < \frac{\mu_1}{\mu_2} < \frac{d-b}{a-b} \text{ and } \frac{c(r-a)}{r(d-b)+s(a-d)} > 1.$$

□

Remark 3.3. If the equilibrium point E_0 is stable, then E_1, E_2, and E_4 do not exist. Also, if E_1 exists, then E_0 is not stable. If E_1 is stable, then the other equilibria do not exist, and vice versa. This is the case for all of the equilibria, i.e., if one equilibrium point exists, then the others do not exist.

3.4. Global stability analysis

We study the global stability of the equilibria by applying appropriate Lyapunov functions and conducting a Lyapunov analysis. We also apply La Salle's invariant principle [16] to determine global stability.

Theorem 3.4. *For the system* (2.1),

(i) *the equilibrium* E_0 *is globally asymptotically stable if* $\mu_1 > 1$ *and* $\mu_2 > 1$;
(ii) *the equilibrium point* E_1 *is globally asymptotically stable if* $\mu_1 > 1$ *and* $\mu_1 > \frac{2+s-b-d}{2}$;
(iii) *the equilibrium point* E_2 *is globally asymptotically stable if* $\mu_2 = 1$, $\frac{s}{c(s-1)} > 1$, *and* $\frac{s}{r-a} > 1$;
(iv) *the equilibrium point* E_3 *is globally asymptotically stable if* $\frac{a-r+1}{2(s-b-1)} > 1$;
(v) *the equilibrium point* E_4 *is globally asymptotically stable if* $\frac{2c+b}{c+s} < \mu_1 < \frac{sad-2brd}{r(c-d+b)-a(c+s)}$.

Proof.

(i) Consider the following Lyapunov function

$$V(x, y, v) = x + y + v.$$

Clearly, V is a positive definite function. Computing the derivative of V along the solutions of model (2.1), we get

$$V' = (r - a)x + (s - b)y - rx^2 - rxy - syx - sy^2 - dv.$$

If $r < a$ and $s < b$, then $V' \leqslant 0$ and $V' = 0$ if and only if $x = y = v = 0$. Thus, the largest invariant set in $\{(x, y, v) \in \Omega : V' = 0\}$ is E_0. Hence, by La Salle's invariance principle [16], E_0 is globally asymptotically stable.

(ii) Define the Lyapunov function $V(x, y, v) = \frac{1}{r}(x - x_1 - x_1 \ln \frac{x}{x_1}) + y + v$. Computing the derivative of V along the solutions to the model (2.1) and collecting like terms

$$V' = x(1 + x_1 - \frac{a}{r}) + y(x_1 + s - b) + v(x_1 - d) - xy - xv + x_1(\frac{a}{r} - 1) - syx - sy^2 - syv - x^2.$$

We note that

$$V' \leqslant x(1 + x_1 - \frac{a}{r}) + y(x_1 + s - b) + v(x_1 - d) + x_1(\frac{a}{r} - 1),$$

if $\mu_1 \geqslant 1$ and $\mu_1 > \frac{2+s-b-d}{2}$. Also, $V' = 0$ if $x = 1 - \frac{a}{r}$ and $y = v = 0$. Thus, the largest invariant set in $\{(x, y, v) \in \Omega : V' = 0\}$ is E_1. Hence, by La Salle's principle, E_1 is globally asymptotically stable.

(iii) Define the Lyapunov function as

$$V(x,y,v) = x + \frac{1}{s}(y - y_2 - y_2 \ln \frac{y}{y_2}) + v.$$

Differentiating and collecting the like terms

$$V' = (r - a - s + y_2)x + (1 + y_2 - \frac{b}{s})y + (y_2 - d + \frac{c}{s}y_2)v + (c - 1 - \frac{c}{s})yv + (\frac{b}{s} - 1)y_2 - rx^2 - rxy - rxv - y^2,$$

where $y_2 = 1 - \frac{b}{s}$. Note that

$$V' \leqslant (r - a - s + y_2)x + (1 + y_2 - \frac{b}{s})y + (y_2 - d + \frac{c}{s}y_2)v + (c - 1 - \frac{c}{s})yv + (\frac{b}{s} - 1)y_2.$$

Thus, $V' \leqslant 0$ if $\mu_2 = 1$, $\frac{s}{c(s-1)} \geqslant 1$, and $\frac{s}{r-a} \geqslant 1$. Also, $V' = 0$ if $x = 0$, $y = 1 - \frac{b}{s}$, and $v = 0$. Thus, the largest invariant set in $\{(x,y,v) \in \Omega : V' = 0\}$ is E_2. Hence, by La Salle's principle, E_1 is globally asymptotically stable.

(iv) Define the Lyapunov function

$$V(x,y,v) = x + y - y_3 - y_3 \ln \frac{y}{y_3} + \frac{1}{v_3}(v - v_1 - v_3 \ln \frac{v}{v_3}),$$

where $y_3 = \frac{d}{c}$ and $v_3 = \frac{sc-bc-ds}{s+c}$. Differentiating and grouping coefficients of the positive terms

$$\begin{aligned} V' &= (r - a - sy_3)x + (s + sy_3 - b - c)y + (sy_3 + cy_3 - \frac{d}{v_3})v + (\frac{c}{v_3} - s - c)yv + +(by_3 - sy_3 + d) \\ &\quad - rx^2 - rxy - rxv - syx - sy^2, \\ &\leqslant (r - a - sy_3)x + (s + sy_3 - b - c)y + (sy_3 + cy_3 - \frac{d}{v_3})v + (\frac{c}{v_3} - s - c)yv + (by_3 - sy_3 + d). \end{aligned}$$

Note that $V' \leqslant 0$ if $\frac{sd}{c(a-r)} \leqslant 1$, $\frac{sd}{c(b-s+c)} \leqslant 1$, $\frac{sc-bc-sd}{c} \leqslant 1$, $\frac{s}{c+b} \geqslant 1$, and $\frac{sc-bc-sd}{c} \geqslant 1$. Combining these conditions, we get the following condition for global stability of E_3,

$$\frac{a - r + 1}{2(s - b - 1)} \geqslant 1.$$

Also $V' = 0$ at E_3. Moreover, the largest invariant set in $\{(x,y,v) \in \Omega : V' = 0\}$ is E_3. Hence, by La Salle's invariance principle, E_3 is globally asymptotically stable.

(v) Define the Lyapunov function

$$V(x,y,v) = \frac{1}{r}(x - x_2 - x_2 \ln \frac{x}{x_2}) + \frac{1}{s}(y - y_2 - y_2 \ln \frac{y}{y_2}) + \frac{1}{s}(v - v_2 - v_2 \ln \frac{v}{v_2}),$$

where $E^* = (x_2, y_2, v_2)$. Differentiating and grouping coefficients of the positive terms

$$\begin{aligned} V' &= (1 + x_2 + y_2)x + (1 + x_2 + y_2)y + (x_2 + y_2 + \frac{c}{s}y_2)v + (\frac{a}{r}x_2 + \frac{b}{s}y_2 + \frac{dv_2}{s}) - x^2 - xy - xv \\ &\quad - \frac{a}{r}x - x_2 - yx - y^2 - \frac{b}{s}y - y_2 - \frac{d}{s}v - \frac{c}{s}v_2 y. \end{aligned}$$

We find that $V' \leqslant 0$ if $\frac{2c+b}{c+s} \leqslant \mu_1 \leqslant \frac{sad-2brd}{r(c-d+b)-a(c+s)}$. Thus under this condition, the equilibrium E_4 is globally stable. Also, $V' = 0$ at E_4, which is the largest invariant set in $\{(x,y,v) \in \Omega : V' = 0\}$. □

4. Numerical analysis

4.1. Numerical simulations

To illustrate our theoretical results, we use Matlab software with the Runge-Kutta method of order 4 to perform simulations for the solutions of the system (2.1). We may change certain parameter values of the parameters to satisfy the existence and stability constraints of each equilibrium point. However, those values must obey the stability conditions.

In light of the parameters' values in Table 1, we use the following parameter variations, $r = 0.3, a = 0.5, s = 0.2, b = .3, d = 0.1$, and $c = 1.2$, to show that the solution curves approach the trivial equilibrium point $E_0 = (0, 0, 0)$ as t approaches infinity. This choice of parameter values is compatible with the stability conditions of E_0, namely $r < a$ and $s < b$. Thus, Figure 1 shows that E_0 is locally asymptotically stable.

For the cancer extinction equilibrium point E_1, we use the parameter values $r = 0.5, a = 0.2, s = 0.3, b = 0.2, d = 0.1$, and $c = 1.2$. So we have $E_1 = (0.6, 0, 0)$ and the solutions are locally asymptotically stable as shown in Figure 2. Note that there are two cases for the parameter values according to stability conditions of E_1. The first case is when $\mu_1 < \mu_2 < 1$ and the other case is $\mu_1 < 1 < \mu_2$. The parameter values above are compatible with the first case. However, if you choose $b = 1$ and $s = 0.1$, then the second case holds. However, the dynamic behavior for the solutions stays the same.

The equilibrium point E_2 is asymptotically stable as shown in Figure 3. The parameter values that obey the stability conditions are $a = 0.2$, $r = 0.5$, $s = 0.5$, $b = 0.1$, $c = 5$, and $d = 4$. The stability is shown in Figure 3 where $E_2 = (0, 0.5, 0)$. Unlike simulations in Figures 1 and 2 where dynamics depend only on a, r, b, and s, the simulations depend on parameter values of the proliferation rate and death rate of the infected cells, c and d, respectively, as well.

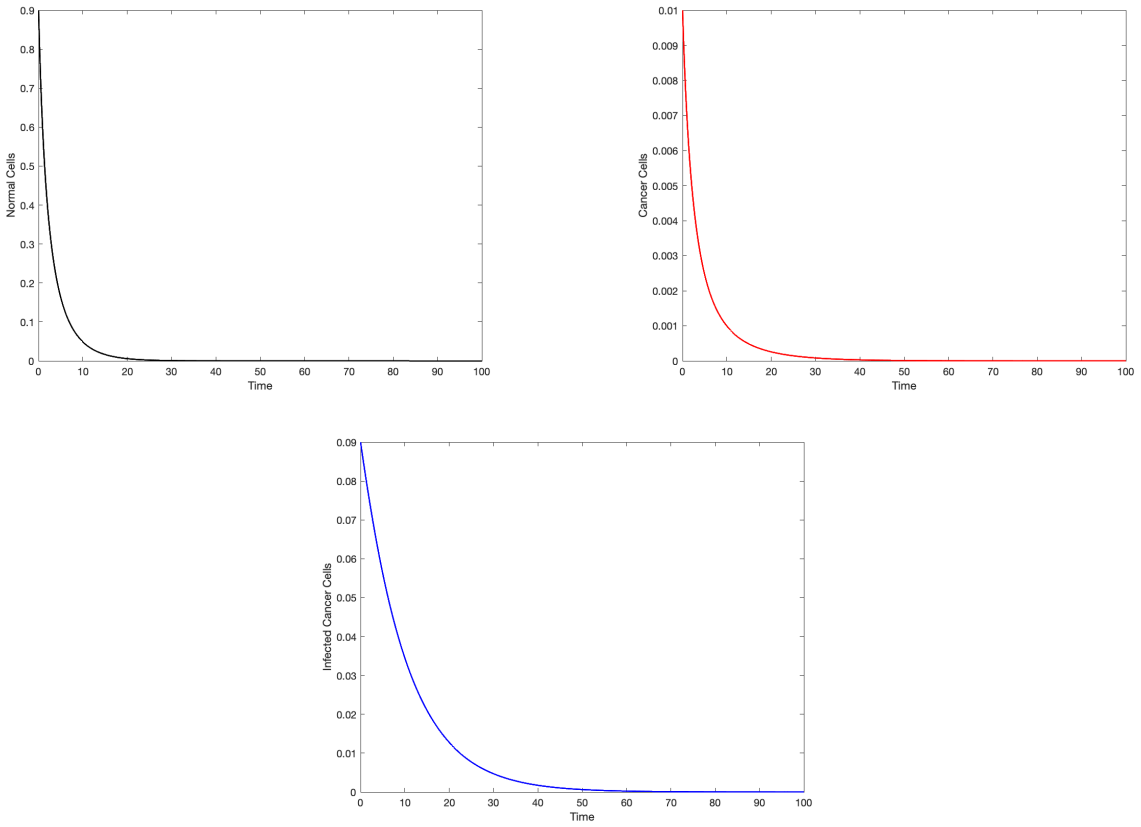

Figure 1: Dynamics of the model with initial values $x = 0.9$, $y = 0.01$, and $v = 0.09$. This figure shows that E_0 is asymptotically stable.

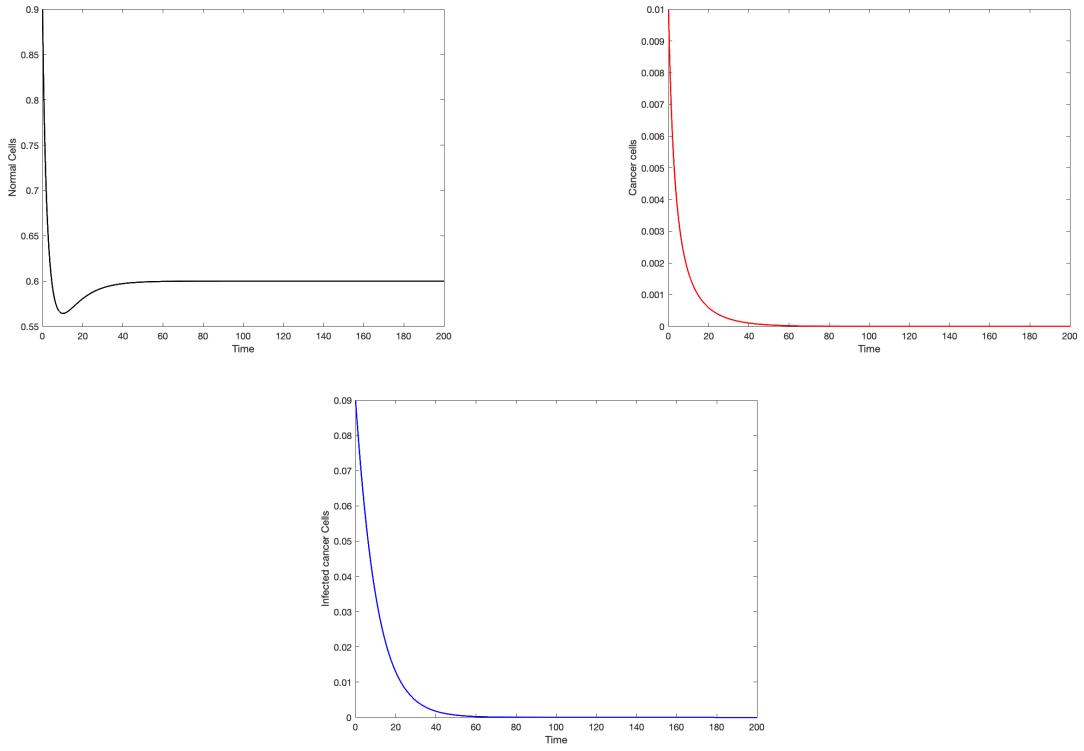

Figure 2: Dynamics of the model with initial values $x = 0.9$, $y = 0.01$, and $\nu = 0.09$. This figure shows that E_1 is asymptotically stable.

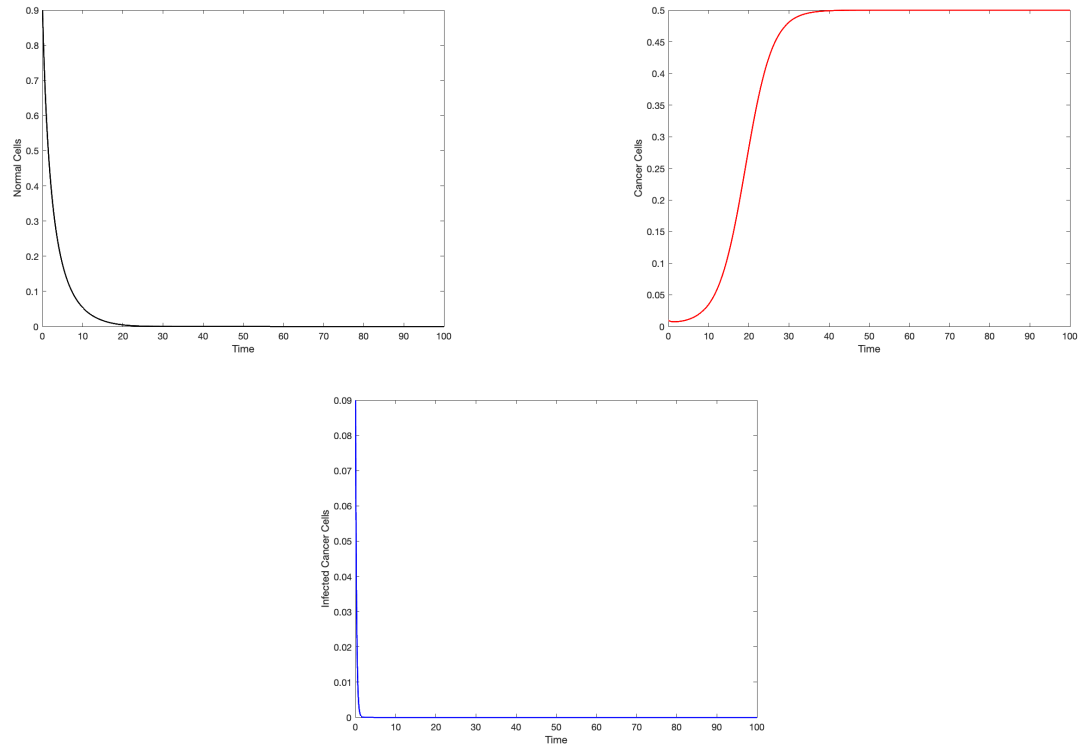

Figure 3: Dynamics of the model with initial values $x = 0.9$, $y = 0.01$, and $\nu = 0.09$. This figure shows that E_2 is asymptotically stable.

The equilibrium point E_3 is locally asymptotically stable as shown in Figure 4. The parameter values are $a = 0.6$, $r = 0.3$, $b = 0.3$, $s = 0.8$, $c = 5$, and $d = 0.4$. The solutions tend to the point $E_3 = (0, 0.08, 0.07514)$ asymptotically. Cancer and infected cancer populations oscillate during the first 200 days, then they stable after that. However, the population of normal cells will die out. Also, simulations of E_2 depend on all parameter values.

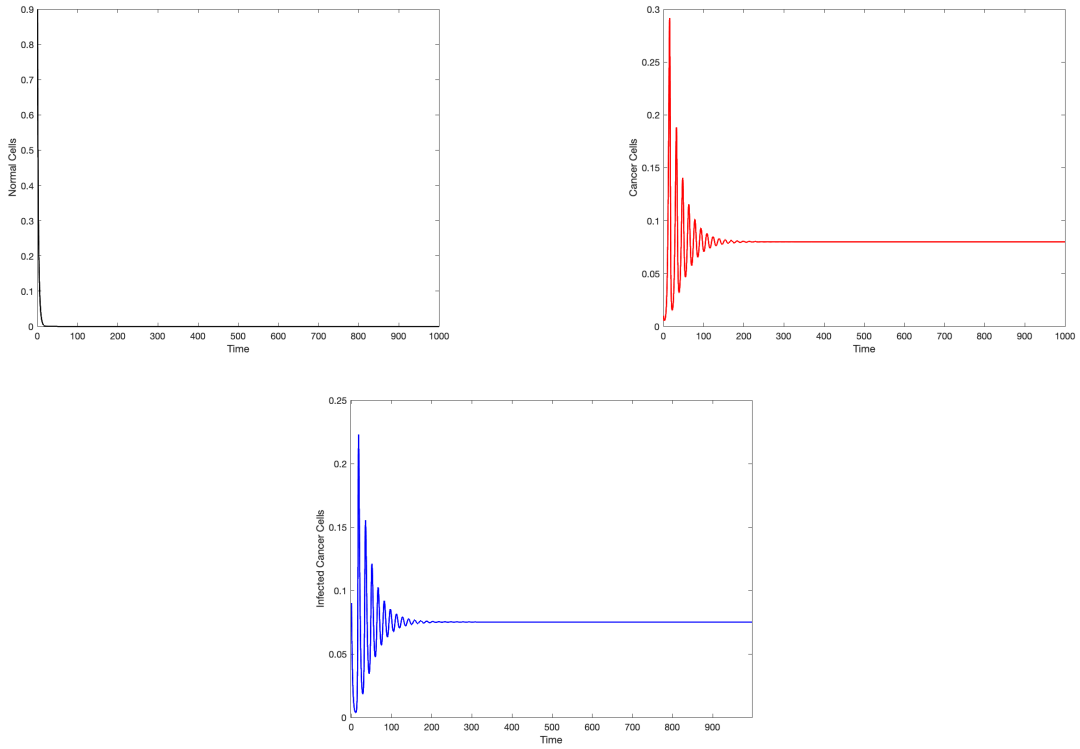

Figure 4: Dynamics of the model with initial values $x = 0.9$, $y = 0.01$, and $v = 0.09$. This figure shows that E_3 is asymptotically stable.

For the equilibrium point E_4, we choose parameter values that make the two local asymptotic conditions valid. We choose $a = 0.4$, $r = 0.5$, $b = 0.3$, $s = 0.4$, $c = 5$, and $d = 0.6$. We choose the initial values $x = 0.05$, $y = 0.05$, and $v = 0.05$. In this case, the solutions will converge to $E_4 = (0.076, 0.12, 0.004)$ as shown in Figure 5.

4.2. Sensitivity analysis

In this section, we conduct a sensitivity analysis on our model to determine parameters that have a high impact on the threshold $\mathcal{R}_O$ and should be targeted by intervention strategies. This analysis allows us to measure the relative change in a variable when a parameter changes. However, the sensitivity has the drawback that it does not give the change of the quantity $\mathcal{R}_0$ relative to the size of the quantity. To address this issue, elasticity of the reproduction number $\mathcal{R}_0$ can be used and defined as follows

$$\mathcal{E}^{p}_{\mathcal{R}_O} = \frac{\partial \mathcal{R}_0}{\partial p}\frac{p}{\mathcal{R}_0},$$

where p is a parameter [16]. The magnitude of the elasticity indices depends generally on the parameter values found in the expression of $\mathcal{R}_O$.

Using parameter values from Table 2, the rate of change of $\mathcal{R}_0$, with respect to one parameter at a time is as follows:

$$\frac{\partial \mathcal{R}_0}{\partial s} = \frac{cb}{s^2 d} > 0, \quad \frac{\partial \mathcal{R}_0}{\partial b} = \frac{-c}{sd} < 0, \quad \frac{\partial \mathcal{R}_0}{\partial c} = \frac{s-b}{sd} > 0, \quad \frac{\partial \mathcal{R}_0}{\partial d} = \frac{-c(s-b)}{sd^2} < 0. \tag{4.1}$$

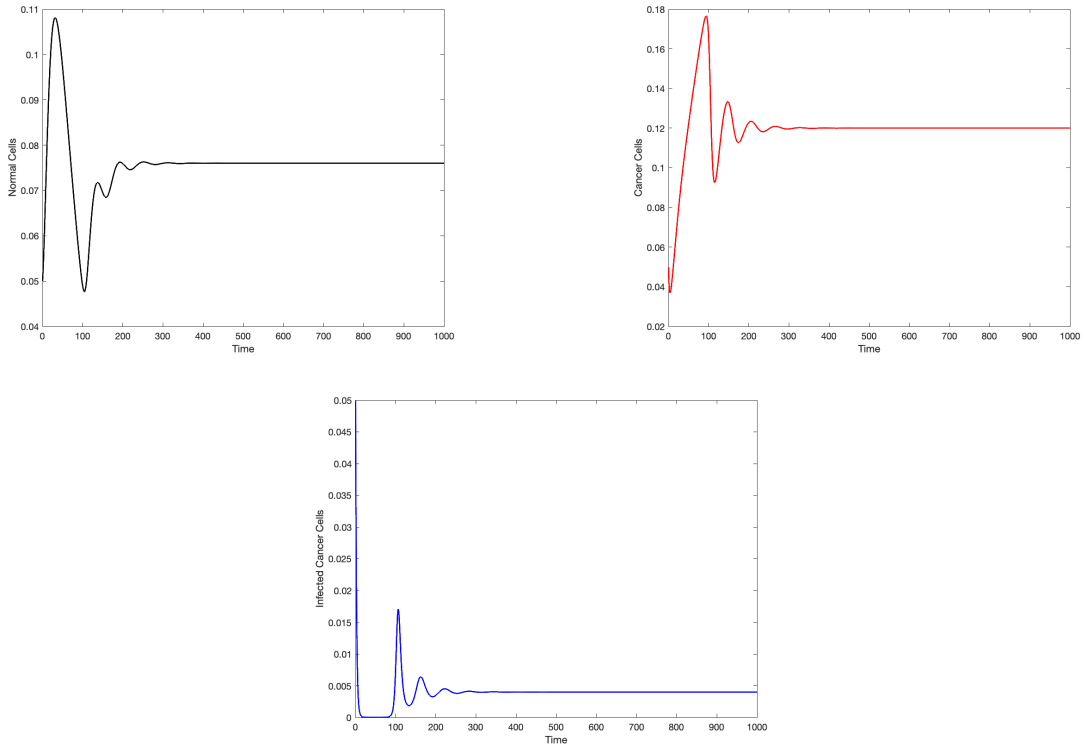

Figure 5: Dynamics of the model with initial values $x = 0.05$, $y = 0.05$, and $v = 0.05$. This figure shows that E_4 is asymptotically stable.

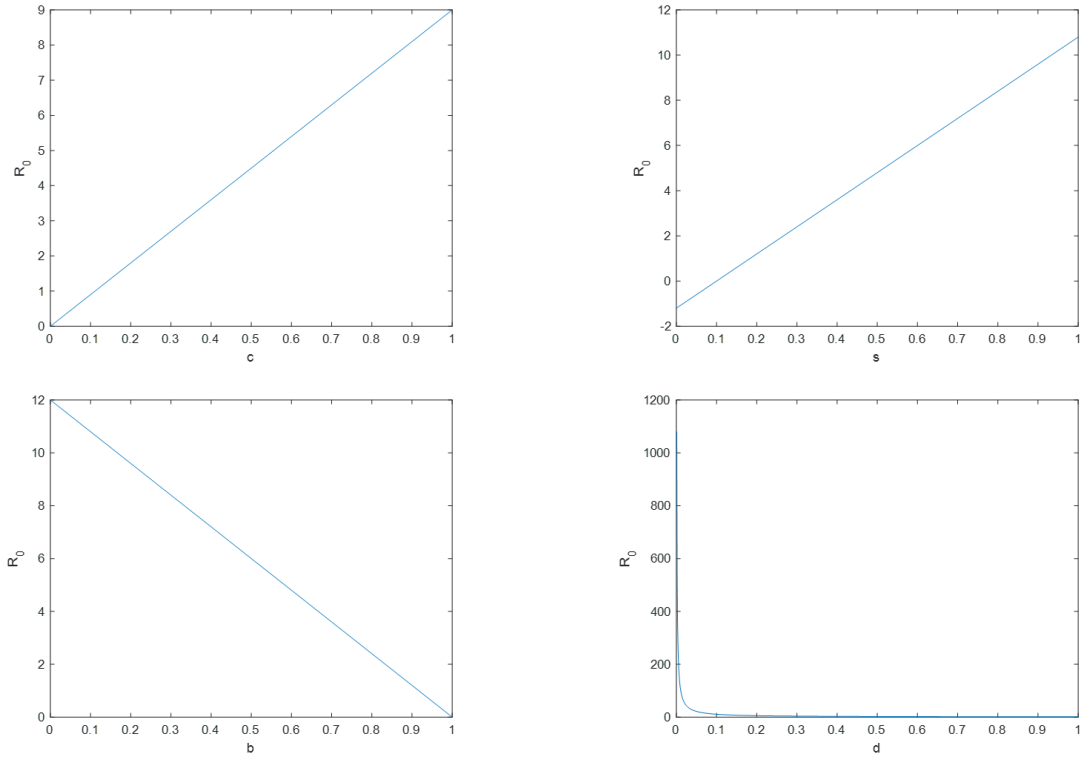

Figure 6: The sensitivity of $\mathcal{R}_0$ with respect to the parameters of the model (2.1).

Table 2: Sensitivity of $\mathcal{R}_0$ evaluated for the parameter values given in Table 1.

Parameter	Elasticity Index value
s	0.111
b	-0.111
c	1.000
d	-1.000

Equation (4.1) shows that $\mathcal{R}_0$ decreases when the parameter values of b and d increase. On contrast, $\mathcal{R}_0$ increases when s and c increase as in Fig 6.

The elasticity indices values shown in Table 2 indicate that the two parameters c and d are the most critical parameters of the model in calculating $\mathcal{R}_0$. That is, the higher the proliferation of the infected cells and the lower the death rate of the infected cells, the higher the number of cancer cells. As a consequence, virotherapy will fail under these changes. It is notable that the other parameters, namely, b and s are not much influential in calculating $\mathcal{R}_O$.

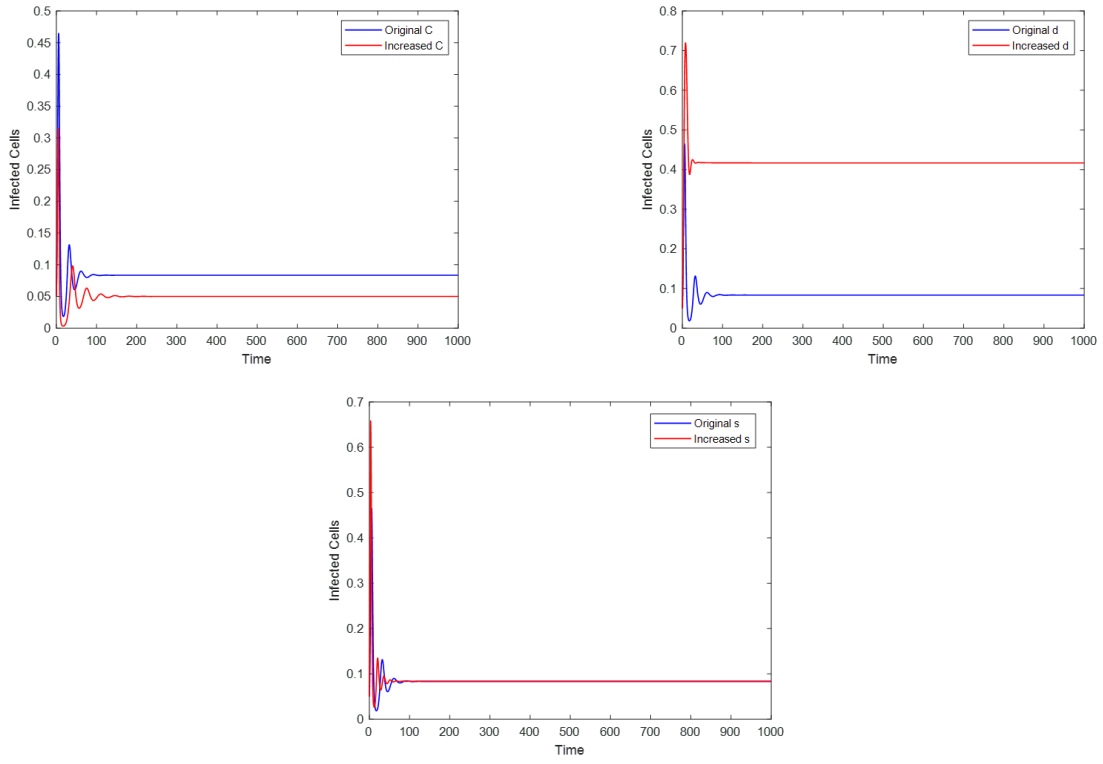

Figure 7: The left figure shows the impact of variation of the parameter c in the number of infected cells y (there is a visible difference). The right figure shows the impact of variation of parameter s in the number of the infected cells y (no visible difference)

Figure 6 shows (left figure) a visible difference in the number of infected cells as the parameter c has changed from the original value 1.2 to a new value $c = 2$. The figure also shows (right figure) that there is no significant change in the number of infected cells if we change the parameter s from the original value $s = 1$ to the new value $s = 2$. This agrees with the elasticity index from Table 2.

5. Discussion and conclusions

In this paper, we studied a model of oncolytic virotherapy that was developed in the studies [4, 5] to describe the virus-cancer cells interaction. In our work, we studied the qualitative properties of the

solutions and used the obtained results to complement and extend the other studies. We hope that our study can lead to a better understanding of the interaction between virus cells and cancer cells.

In the above references, it is proved that a high virus clearance rate can result in treatment failure. However, decreasing the virus clearance rate slightly while keeping the other parameter values unchanged results in treatment success. This agrees with the result obtained in [5].

Our study shows that when $\mu_1 < 1$, and if $\mu_1 < \mu_2$, then the treatment is successful regardless of the values of the proliferation and death of the virus, i.e., c and d, respectively. This result seems to agree only partially with the result obtained in [4, 5], and thus it is worth focusing on. This result is shown in Figure 2 where the solutions converge to the cancer extinction equilibrium E_1, where we notice that once cancer is extinct, the virus population will follow soon.

When $\mu_2 < \mu_1$, $\mu_2 < 1$, and if $\mathcal{R}_0 < 1$, then the viruses will extinct and the normal cells will follow. In this case, the disease will be dominant and the treatment fails. The virus-infected cells go extinct and the tumor cells will occupy the simulation space as tumor cells grow faster than normal cells E_2. Mathematically, solutions will converge to E_2 as shown in Figure 3. Unlike simulations of the equilibrium solutions E_0 and E_1, the dynamics depend on the values of the parameters c and d and this agrees with the stability conditions of our study.

Under the conditions in Theorem 3.2 (iv), the solutions oscillate at the beginning of the therapy, then they tend to be stable as shown in Figure 4. At the cancer-virus equilibrium E_3, normal cells die out leaving cancer cells and virus-infected cells with stable population sizes. This is another case where therapy is not successful since normal cells are completely destroyed and tumor cells and infected tumor cells coexist E_3.

The equilibrium point E_4 exists and is asymptotically stable under the conditions of Theorems 3.2 and 3.4. The three populations will coexist with nonzero stable sizes of E_4. Figure 5 shows all populations tend to a stable behavior after approximately 200 days of the treatment.

Finally, the trivial equilibrium point E_0 is reached when both the ratio of the death rate of normal cells to the proliferation rate, μ_1 and the ratio of the death rate of cancer cells to their growth rate are less than one. All populations die out E_0 as shown in Figure 1.

While studying virotherapy is still in the beginning stages, at least mathematically and clinically, studying and modifying different models of virotherapy is necessary to understand the dynamics of the treatment and to optimize it. We believe that the results and observations of this paper can lead to a better understanding of virotherapy especially the interaction between infected tumor cells and uninfected tumor cells.

One of the questions we tried to address is what range of virus parameters can maximize the chance for successful therapy. In our study, we showed how the dynamics of model (2.1) are largely dependent on specific parameter values of replication and death rates of normal and cancer cells, r, a, and s, b, respectively. Those critical virus parameters that we denoted as μ_1 and μ_2 can result in qualitatively different dynamics of the model (2.1). However, varying the virus replication c and death rate of virus d can only affect the dynamics of the equilibrium points E_2, E_3, and E_4.

The sensitivity analysis conducted in Section 5 shows that the parameters c and d are the most influential parameters on the basic reproduction number. This agrees with the results we obtained from the qualitative analysis of the equilibria.

As a possible future research, some dynamical behavior cannot be explained well from the deterministic model, especially when solutions start to approach zero after a specific time. Therefore incorporating some stochastic effects can produce a different behavior starting from that moment.

Acknowledgment

The authors would like to thank Concord University for funding this research.

References

[1] A. Abu-Rqayiq, *Mathematical Modeling & Dynamics of Oncolytic Virotherapy*, In: Advances in Precision Medicine Oncology, Intechopen Publisher, U.K., (2021). 1

[2] A. Abu-Rqayiq, M. Zannon, *On the dynamics of fractional-order oncolytic virotherapy models*, J. Math. Comput. Sci., **20** (2020), 79–87. 1

[3] Z. Bajzer, T. Carr, K. Josić, S. J. Russell, D. Dingli, *Modeling of cancer virotherapy with recombinant measles viruses*, J. Theoret. Biol., **252** (2008), 109–122. 1

[4] D. R. Berg, *A Flexible Simulator for Oncolytic Viral Therapy*, Master Thesis, University of Minnesota ProQuest Dissertations Publishing, (2015). 1, 1, 2, 2, 5

[5] D. R. Berg, C. P. Offord, I. Kemler, M. K. Ennis, L. Chang, G. Paulik, Z. Bajzer, C. Neuhauser, D. Dingli, *In vitro and in silico multidimensional modeling of oncolytic tumor virotherapy dynamics*, PLoS Comput. Biol., **15** (2019), 1–18. 1, 2, 2, 5

[6] M. Biesecker, J.-H. Kimn, H. Lu, D. Dingli, Ž. Bajzer, *Optimization of virotherapy for cancer*, Bull. Math. Biol., **72** (2010), 469–489.

[7] D. Dingli, M. D. Cascino, K. Josić, S. J. Russell, Ž. Bajzer. *Mathematical modeling of cancer radiovirotherapy*, Math. Biosci., **199** (2006), 55–78. 1

[8] D. Dingli, C. Offord, R. Myers, K.-W. Peng, T. W. Carr, K. Josic, S. J. Russell, Z. Bajzer, *Dynamics of multiple myeloma tumor therapy with a recombinant measles virus*, Cancer Gene Ther., **16** (2009), 873–882. 1

[9] R. Durrett, S. Levin, *Spatial aspects of interspecific competition*, Theor. Popul. Biol., **53** (1998), 30–43. 1

[10] M. El Younoussi, Z. Hajhouji, K. Hattaf, N. Yousfi, *Dynamics of a reaction-diffusion fractional-order model for M1 oncolytic virotherapy with CTL immune response*, Chaos Solitons Fractals, **157** (2022).

[11] G. I. Evan, K. H. Vousden, *Proliferation, cell cycle, and apoptosis in cancer*, Nature, **411** (2020), 342–348. 1

[12] A. Friedman, J. P. Tian, G. Fulci, E. A. Chiocca, J. Wang *Glioma virotherapy: effects of innate immune suppression and increased viral replication capacity*, Cancer Res., **66** (2006), 2314–2319. 1

[13] K. Fujii, *Complexity-stability relationship of two-prey-one-predator species system model: local and global stability*, J. Theoret. Biol., **69** (1977), 613–623. 1, 2

[14] V. Hutson, G. T. Vickers, *A criterion for permanent coexistence of species, with an application to a two-prey one-predator system*, Math. Biosci., **63** (1983), 253—269. 2

[15] E. Kelly, S. J. Russel *History of Oncolytic Viruses: Genesis to Genetic Engineering*, Mol. Ther., **15** (2007), 651–659. 1

[16] M. Martcheva, *An Introduction to Mathematical Epidemiology*, Springer, New York, (2015). 3.2, 3.4, 3.4, 4.2

[17] C. Offord, Z. Bajzer *A hybrid global optimization algorithm involving simplex and inductive search*, Lect. Notes Comput. Sci., **2074** (2001), 680–688.

[18] H. T. Ong, M. M. Timm, P. R. Greipp, T. E. Witzig, A. Dispenzieri, S. J. Russell, K.-W. Peng, *Oncolytic measles virus targets high CD46 expression on multiple myeloma cells*, Exp. Hematol., **34** (2006), 713–720. 2

[19] L. R. Paiva, C. Binny, S. C. Ferreira, Jr., M. L. Martins, *A multiscale mathematical model for oncolytic virotherapy*, Cancer Res., **69** (2009), 1205–1211.

[20] T. A. Phan, J. P. Tian, *The Role of the Innate Immune System in Oncolytic Virotherapy*, Comput. Math. Methods Med., **6** (2017), 1–17. 1

[21] C. L. Reis, J. M. Pacheco, M. K. Ennis, D. Dingli, *In silico evolutionary dynamics of tumor virotherapy*, Integr. Biol., **2** (2010), 41–45. 2

[22] D. M. Rommelfanger, C. P. Offord, J. Dev, Z. Bajzer, R. G. Vile, D. Dingli *Dynamics of melanoma tumor therapy with vesicular stomatitis virus: explaining the variability in outcomes using mathematical modeling*, Gene Ther., **19** (2012), 543–549. 1

[23] J. P. Tian, *The Replicability of Oncolytic Virus: Defining Conditions in Tumor Virotherapy*, Math. Biosci. Eng., **8** (2011), 841–860. 1

[24] Y. Takeuchi, N. Adachi,*Existence and bifurcation of stable equilibrium in two-prey, one-predator communities*, Bull. Math. Biol., **45** (1983), 877–900. 2

[25] P. Van Den Driessche, J. Watmough, *Reproduction numbers and sub-threshold endemic equilibria for compartmental models of disease transmission*, Math. Biosci., **180** (2002), 29–48.

[26] L. M. Wein, J. T. Wu, D. H. Kirn, *Validation and analysis of a mathematical model of a replication-competent oncolytic virus for cancer treatment: Implications for virus design and delivery*, Cancer Res., **63** (2003), 1317–1324.

[27] D. Wodarz, *Viruses as antitumor weapons: defining conditions for tumor remission*, Cancer Res., **61** (2001), 3501–3507. 1

[28] D. Wodarz, *Gene Therapy for Killing p53-Negative Cancer Cells: Use of Replicating Versus Nonreplicating Agents*, HUM. Gene Ther., **14** (2003), 153–159. 1, 3.2

[29] D. Wodarz, *Computational approaches to study oncolytic virutherapy: insights and challenges*, Gene Ther. Mol. Biol., **8** (2004), 137–146.

[30] D. Wodarz, A. Hofacre, J. W. Lau, Z. Sun, H. Fan, N. L. Komarova, *Complex spatial dynamics of oncolytic viruses in vitro: mathematical and experimental approaches*, PLoS Comput. Biol., **8** (2012), 1–8. 1

[31] D. Wodarz, N. Komarova, *Towards predictive computational models of oncolytic virus therapy: Basis for experimental validation and model selection*, PLoS One, **4** (2009), 1–9.

[32] J. T. Wu, H. M. Byrne, D. H. Kirn, L. M. Wein, *Modeling and analysis of a virus that replicates selectively in tumor cells*, Bull. Math. Biol., **63** (2001), 731–768.

[33] J. T. Wu, D. H. Kirn, L. M. Wein *Analysis of a three-way race between tumor growth, a replication-competent virus, and an immune response*, Bull. Math. Biol., **66** (2004), 605–625. 1